Wave and Circulation Prediction on Unstructured Grids

Joannes J. Westerink
Department of Civil Engineering and Geological Sciences
Fitzpatrick Hall of Engineering
University of Notre Dame
Notre Dame, IN 46556
phone: (574) 631-6475 fax: (574) 631-9236 email: jjw@photius.ce.nd.edu

Clint Dawson
Department of Aerospace and Engineering Mechanics
Institute for Computational Engineering and Sciences
The University of Texas at Austin
1 University Station C0200
Austin, TX 78712
phone: (512) 475-8627 fax: (512) 471-8694 email: clint@ices.utexas.edu

Rick A. Luettich
University of North Carolina at Chapel Hill
Institute of Marine Sciences
3431 Arendell Street
Morehead City, NC 28557
phone: (252) 726-6841 ext. 137 fax: (252)726-2426 email: rick_luettich@unc.edu

Award Number: N00014-06-1-0285
http:// www.nd.edu/~adcirc

LONG TERM GOALS

The long term goal of this research is to significantly advance computational methods for multi-scale flow physics in geometrically and/or hydrodynamically complex oceanic and coastal ocean environments, through refinements in the defined physics, domain definition and computational grid resolution. The particular focus is on improved coupling of wind generated short wave and circulation models within the framework of adaptive, unstructured grid models for oceanic and coastal waters.

OBJECTIVES

The objective of this project is the dynamic coupling of the ADCIRC circulation model and the short wind wave model SWAN using unstructured adaptive computational meshes. In recent experience with coupling the continuous Galerkin based version of ADCIRC with short wind wave models, it has been found that wave transformation zones require high levels of resolution in order to correctly capture the wave radiation stress forcing to the circulation model. However the wave transformation zone tends to shift depending on the direction and period of the waves. Thus *hp*-adaptive discontinuous Galerkin (DG) based solutions are being developed to optimize the application of high resolution zones to correctly capture the wave coupling within these zones without over-resolving adjacent areas.

Report Documentation Page

Form Approved
OMB No. 0704-0188

1. REPORT DATE	2. REPORT TYPE	3. DATES COVERED
30 SEP 2007	**Annual**	**00-00-2007 to 00-00-2007**

4. TITLE AND SUBTITLE	5a. CONTRACT NUMBER
Wave And Circulation Prediction On Unstructured Grids	5b. GRANT NUMBER
	5c. PROGRAM ELEMENT NUMBER
6. AUTHOR(S)	5d. PROJECT NUMBER
	5e. TASK NUMBER
	5f. WORK UNIT NUMBER
7. PERFORMING ORGANIZATION NAME(S) AND ADDRESS(ES) **University of Notre Dame,Department of Civil Engineering and Geological Sciences,Notre Dame,IN,46556**	8. PERFORMING ORGANIZATION REPORT NUMBER
9. SPONSORING/MONITORING AGENCY NAME(S) AND ADDRESS(ES)	10. SPONSOR/MONITOR'S ACRONYM(S)
	11. SPONSOR/MONITOR'S REPORT NUMBER(S)

12. DISTRIBUTION/AVAILABILITY STATEMENT
Approved for public release; distribution unlimited

13. SUPPLEMENTARY NOTES
code 1 only

14. ABSTRACT

15. SUBJECT TERMS

16. SECURITY CLASSIFICATION OF:			17. LIMITATION OF ABSTRACT	18. NUMBER OF PAGES	19a. NAME OF RESPONSIBLE PERSON
a. REPORT **unclassified**	b. ABSTRACT **unclassified**	c. THIS PAGE **unclassified**	**Same as Report (SAR)**	**22**	

APPROACH

We have focused on three areas to accomplish the defined objectives. The first area is implementing and evaluating *hp*-adaptive schemes for DG solutions to the shallow water equations (SWE) in anticipation of coupling with a mesh adaptive version of the SWAN wave model which is under development. This will improve the unstructured grid capabilities for the ADCIRC circulation model by implementing *hp*-adaptive methods to ensure that sufficient grid resolution is provided for all relevant flow scales. The present implementation of ADCIRC is based on both Continuous Galerkin (CG) and DG finite element methods. Currently we are intensively developing the DG based algorithms. DG algorithms are particularly well-suited for both propagation and advection dominated problems with or without sharp gradients in the forcing function, bathymetry, and/or flow. DG methods inherently preserve mass perfectly on an elemental level, which make them ideal for coupling flow and transport models. Example problems include flows with strong eddies such as those issuing from and through inlets; flows through rapidly varying bathymetry such as canyons or deep scour holes in inlets; and flows with sharp fronts such as tidal bores, ebb tide – waves interactions in inlets and wetting fronts. DG methods are conceptually similar to finite volume methods although DG methods are readily implemented with higher-order bases. DG methods are also ideal since non-conforming *h* and *p* refinement and adaptivity can be implemented. In addition, DG methods are significantly more accurate on a per degree of freedom basis than CG methods. Finally DG based methods require less message passing within a parallel framework and are therefore more suitable for massively parallel processing.

The second area is evaluating the influence of grid resolution in the SWE circulation model in relation to the wind-wave model in the computed wave radiation stress set up. In addition, we are studying the sequencing of interpolation and the wave radiation stress gradient computation and the influence of both the wave and surge model grids in this context.

The third area is to improve the wave – circulation model coupling which was bottle necked by our single processor interface for communication between the two models. We are designing all paradigms for very large scale parallelism on distributed memory machines, anticipating thousands of processors. We are currently using the globalized output to localized input/interpolation to communicate between the wind wave and circulation models. We are working on a synchronous parallel/parallel interface.

WORK COMPLETED

Work has continued on the DG modeling system development focusing on system validation, improvements in the automated *p*-adaptivity, implementation and testing automated *h*-adaptivity, improvements in parallel coding and scaling, and implementing three dimensional baroclinic terms.

System validation work has focused on basin scale to inlet scale problems to ensure that the DG based algorithms are robust over the entire range of momentum balances and allow the use of large scale domains. Large scale domains are attractive since they significantly improve the coupling mechanisms for deep ocean water to propagate onto the shelf and into inlets and adjacent floodplains for all energetic scales of motion. Validation exercises have focused on tides. Tide simulations include tidal boundary forcing functions and tidal potential functions.

DG development work has advanced significantly. Improvements have been made in the robustness and accuracy of the DG based wetting/drying algorithm, including proving convergence for a range of

problems. The DG code now features both *p*- (polynomial order) and standard *h*- (grid) refinement/adaptivity options. The *p*-adaptivity is made simple with the use of a hierarchical basis and refinement is simply based on adding higher-order basis functions. Derefinement is implemented by discarding higher-order basis functions, equivalent to an L2 projection of solution onto lower order space. A "sensor" proposed by Burbeau and Sagaut (2005) is used to decide where to *p*-refine. The *h* data structure of Demkowicz (2006) has been implemented. This structure stores only minimal mesh information and no information for new elements is stored explicitly whatsoever. Genealogical information stored for element nodes – i.e. children and parents of nodes and element connectivities are then recovered from this information using fast data structure supporting algorithms. The *h*-adaptive algorithm performs standard h4 isometric refinement (Figure 1). The method allows the use of hanging nodes but is limited to so-called 1-irregular meshes (Figure 2). A discontinuity detector is used to decide where to *h*-refine (Krivodonova et al. 2004). Note both the indicators of *h*- and *p*-adaptation are based on quantities that are easy to compute or already available and maintain the local character of the DG method.

Improvements have been made in both the efficiency of the DG code as well as the parallel implementation. Through loop level optimization, we have improved the efficiency of the DG code so that on a per degree of freedom basis it is only 3.5 times more expensive to run than the CG code (compared to 8 times more expensive prior to optimization). It is noted that the DG code is significantly more accurate than CG on a per degree of freedom basis. Parallelization has also been improved so that linear speedups are maintained much longer than CG based methods. Parallelization is achieved through domain decomposition with a shared overlapping layer of element with inter-processor communications based on embedded shared layer elements on one processor sending polynomial expansion coefficients to the corresponding exterior element in the adjacent processor. This allows all computations including the Roe flux computation to be performed on each individual processor.

Since the goal is to develop multi-scale adaptive flow computation capabilities for the entire range of coastal ocean physics and problems, we have also investigated the application of DG methods to three-dimensional, baroclinic models. A three-dimensional DG model was developed by Dawson and Aizinger (2007), and has been extended from barotropic to baroclinic mode. The model uses a *z*-grid with general prismatic elements and has the capability to follow a sloped (piecewise linear) bottom bed. The method is based on the use of discontinuous, piecewise polynomial approximating functions for each primary variable, defined over each element. The primary focus during the past year was the incorporation of various turbulence closure models into the code and the preliminary testing of these models. Turbulence models that were implemented include two algebraic (zeroth order) models, a one equation model, and various two equation models. Results using different orders of approximating spaces, from piecewise constant to piecewise quadratic, indicate that piecewise quadratic approximations of kinetic energy are superior at resolving the boundary layer at the sea bed.

We have investigated vertical eddy viscosity models of various levels of computational and conceptual complexity. In order of increasing complexity those include a constant eddy viscosity coefficient, an algebraic (zeroth order) model, as well as one and two equation models. The simplest model amounts to explicitly specifying diagonal entries to the tensors of eddy viscosity/diffusivity coefficients for all variables. Two algebraic models implemented in our DG code are due to Davies (1986) and give good results at a reasonable computational cost in cases where accurate vertical resolution of flow is not important. The first order vertical eddy viscosity closure model solves a transport equation for the turbulent kinetic energy in addition to the mass, momentum, and species transport equations. The

turbulent mixing length is computed algebraically in this model (see Delft3D-Flow manual, 2005). The second order closure model we implemented is based on the generic turbulence length scale model proposed by Warner et al. (2005). The main advantage of this formulation is the ability to switch between several two equation models, including k-epsilon and Mellor-Yamada, by changing a few constant parameters.

In addition to developing robust basin to channel scale DG based *hp*-adaptive algorithms, we are studying the effects of wave radiation stress induced set up in hurricane environments. Using models developed for the USACE in Southern Louisiana, we are examining the degree of wave set up. We are designing *hp*-adaptivity in order to minimize the high level of resolution in the highly refined broad wave transformation zones that we have built into the current static models.

In the area of inter-model communications we have refined the global to local paradigms and interpolation. We have also improved code efficiency by specializing output processors.

RESULTS

The DG based code has been applied to a domain encompassing the western north Atlantic and the entire Gulf of Mexico and Caribbean Sea. This domain allows tides to interact between basins, be amplified within the resonant Gulf and Caribbean and propagate onto the shelves. The coarse grid applied, shown in Figure 3, works very well with the DG solution as is illustrated in the sample tidal comparisons shown in Figures 3 and 4. A much more nonlinear case is the tide computation in Willapa Bay shown in Figure 5. This case tests the advective terms as well as the new DG wetting/drying algorithm since the tide range is large (more than 4 m), there is a narrow inlet to a large back bay and there are large tidal flats with a significant portion of the bay drying during the tidal cycle. This problem encompasses basin to channel scales. Results at NOS stations are compared to data in Figure 6.

The *p*-adaptive solutions have now been applied to Grays Harbor, a highly advection dominated case characterized by a deep inlet channel and long jetties which are partially submerged. The grid and bathymetric detail is shown in Figures 7 and 8. *p*-adaptivity is shown in Figures 9 and 11 for flood and ebb tides respectively, while the corresponding currents are shown in Figures 10 and 12. We note that eddies as well as the strong shear are nicely picked up by the *p* refinement sensors.

The *h*-adaptive algorithms have been tested on the idealized dam break problem illustrated in Figure 13. The colors indicate surface water elevation. Initially the left and right sides of the basin are at different water levels and a sluice is then instantly opened between the two portions of the basin. It is noted that the shock propagates from the left side to the right side and as it does so the *h*-adaptivity refines the grid to capture the large gradients.

To evaluate the parallel performance of the DG model, we tested a medium size problem and compared the performance to that of our CG based code. The problem consists of the western North Atlantic Ocean, Gulf of Mexico and Caribbean Sea and in the grid contains 492,179 elements and 254,565 nodes. Simulations were performed on the TACC's Lonestar Dell Linux Cluster, which consists of 5,840 cores within 1,460 Dell PowerEdge 1955 blades each with two Xeon 5100 series 2.66GHz dual-core processors. A simulation was performed on 16, 32, 64, 128, 256, 512, and 1024 cores. Figure 14 shows the speedup, defined as the ratio of the wall clock time of a single core run over the wall clock time of a parallel run. For this test case, the ADCIRC-CG code exhibits linear speed-up

to 64 cores but tails off beyond 128 cores. This behavior is expected for problems of fixed size; our experience to date indicates that the code begins to lose parallel efficiency at around 2000 finite element mesh nodes/core. The ADCIRC-DG code scales close to linearly up to 256 processors and continues to scale with efficiency above 50% to 1024 cores. The corresponding efficiency of the CG and DG codes is shown in Figure 15. It is noted that more parallel efficiency improvements are possible for the DG code and that scaling and efficiency improve for larger problems.

As a test run for the three dimensional implementation, we simulate tide-driven flow in the Bight of Abaco. The domain bathymetry and the coarse mesh are shown in Figures 16 and 17. A standard tidal forcing of five constituents was imposed at the open sea boundary. In Figures 18 through 22, we compare the free surface elevation computed using piecewise linear approximation spaces and up to 5 layers in the vertical direction, using algebraic (Figure 18), Delft3D order 1 (Figure 19), k-epsilon (Figure 20), k-omega (Figure 21) and the ``generic'' order 2 model (Figure 22). The results, including those obtained using the algebraic turbulence closure model, are closely matched.

For studying wave radiation stress gradient induced set up, we have been applying the SL15 domain/grid for Southern Louisiana shown in Figures 23-27. This grid was developed for the USACE/FEMA Joint Coastal Surge Study and has very high levels of shelf, coastal and inland resolution in order to compute hurricane storm surge. In addition, as can be seen in Figure 25, a wide swath of high resolution (80m and smaller) has been specified in the coastal wave transformation zone. In fact, about 40% of the 2.17 million computational points resolve the wave transformation zone. The corresponding wave radiation stress high gradient zones for given storms and parts of a specific storm are much narrower than the swaths of high resolution, although the zones shift in time with the storm and wave period. We have been working on the implementation of the DG code and the *hp*-adaptive DG code to this problem. A CG evaluation of wave induced radiation stress for Hurricanes Katrina and Rita indicates that wave radiation stress induced set up along the coast is generally less than 0.5 m and up to 1 m in well focused areas that do not have extensive back-bay areas for the water to spread out. Wave radiation induced set up is less for Rita than for Katrina because of the predominant winds coming off of land during much of the storm. We are systematically going through grid convergence studies to define levels of required resolution.

IMPACT/APPLICATIONS

This work will significantly improve the accuracy of the computed physics for coastal ocean hydrodynamic computations, especially for multi-scale physics since the DG based adaptivity will automatically and optimally sense where the mesh refinement is needed. It will also reduce model development times since base meshes only need to represent the geometry and not the hydrodynamics.

REFERENCES

Aizinger V. and Dawson C., *Computer Methods in Applied Mechanics and Engineering*, 196, 734-746, 2007.

Burbeau and Sagaut, *Computers and Fluids*, 34, 401-417, 2005.

Demkowicz, L., Computing with *hp*-Adaptive Finite Elements, 2006.

Davies, A., *Journal of Physical Oceanography*, 16(5), 797-813, 1986.

Krivodonova, L., Xin, J., Remacle, J.-F. Chevaugeon, N., Flaherty, J.E., *Applied Numerical Mathematics*, 48, 323–338, 2004.

Warner et al, *Ocean Modeling*, 8, pp. 81-113, 2005.

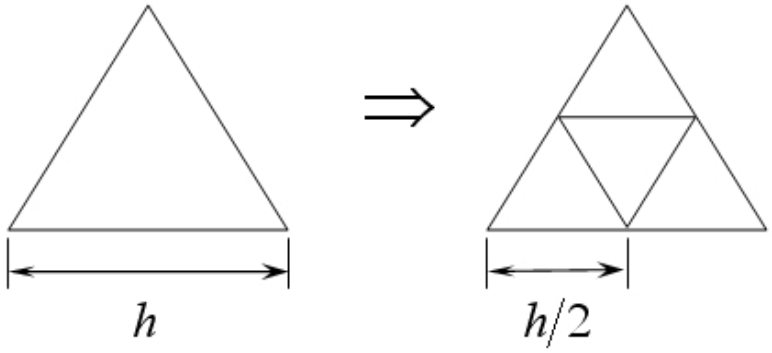

Figure 1: Standard h4 isometric refinement.

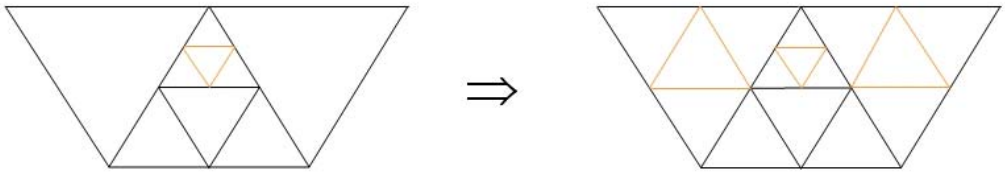

Figure 2: 1-irregular meshes with hanging nodes.

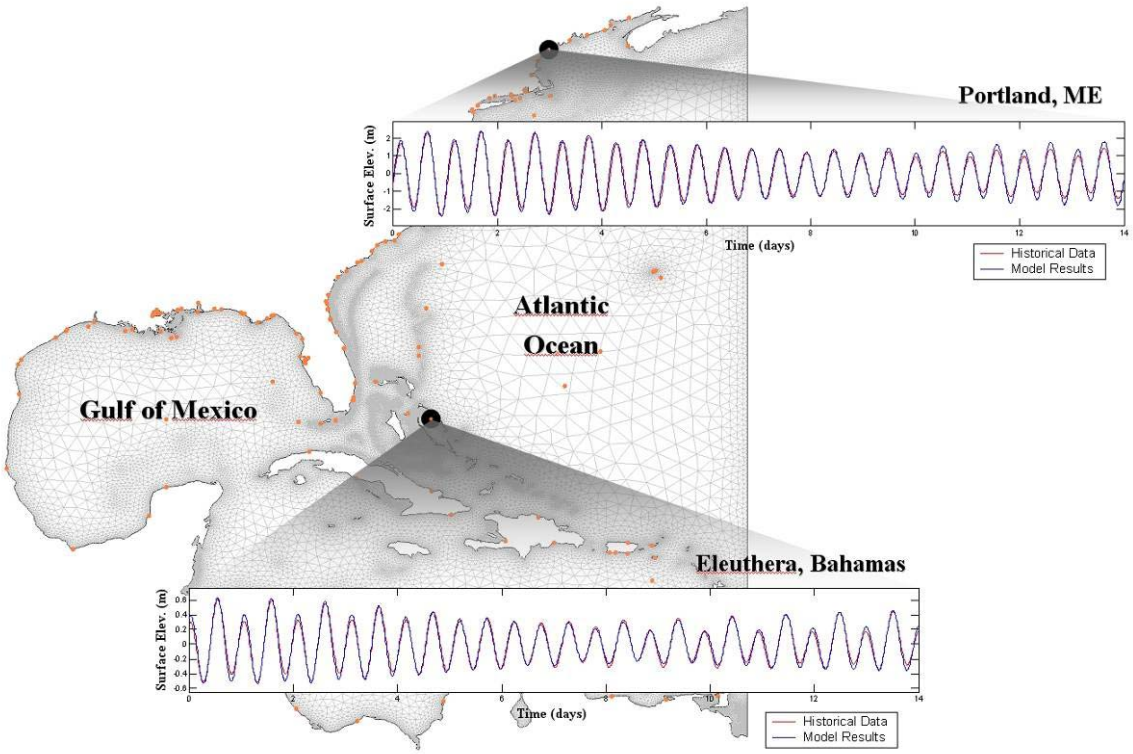

Figure 3: Coarse grid Western North Atlantic domain with sample tide comparisons to Fourier re-synthesized measured tidal data.

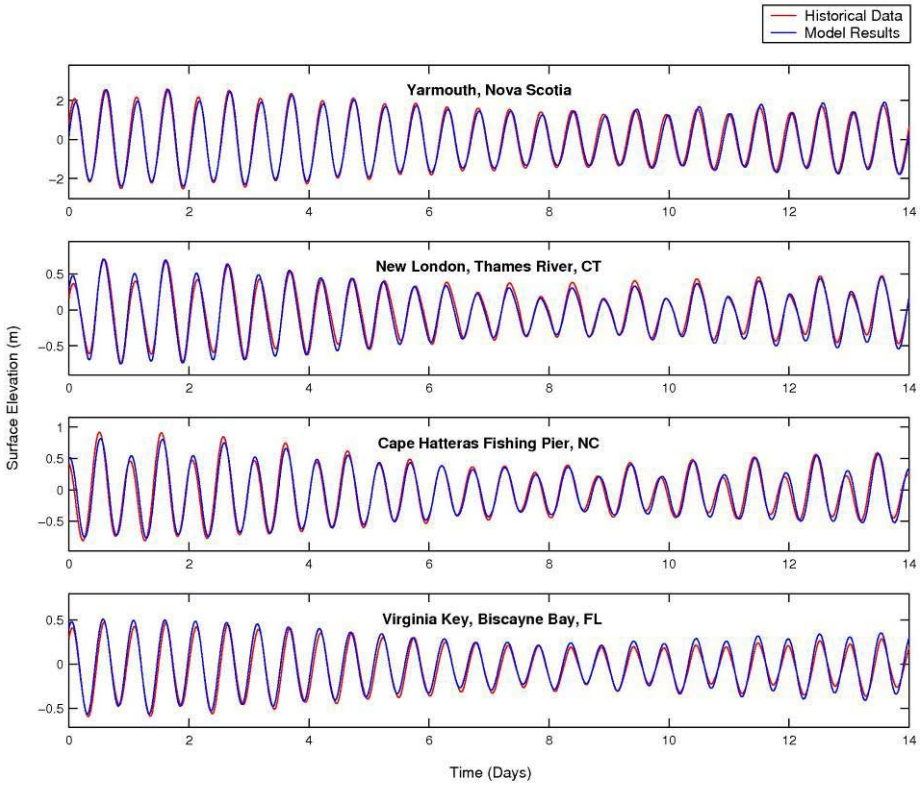

Figure 4: Sample tide comparisons to Fourier re-synthesized measured tidal data along U.S. coastline.

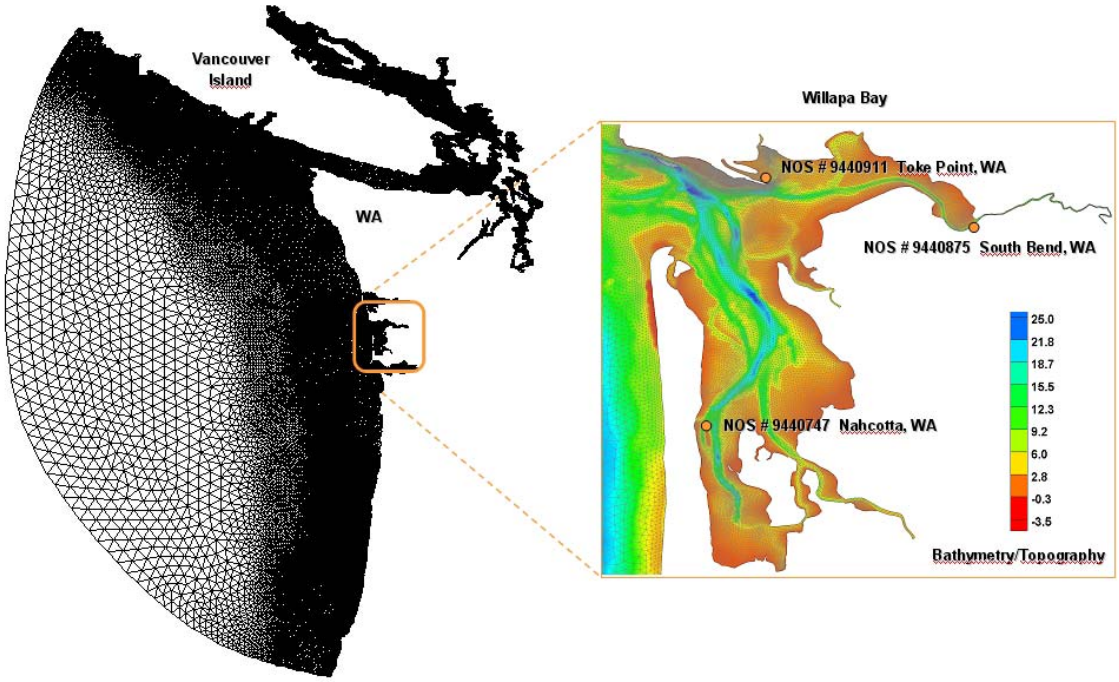

Figure 5: Willapa Bay grid and topography/detail within the bay

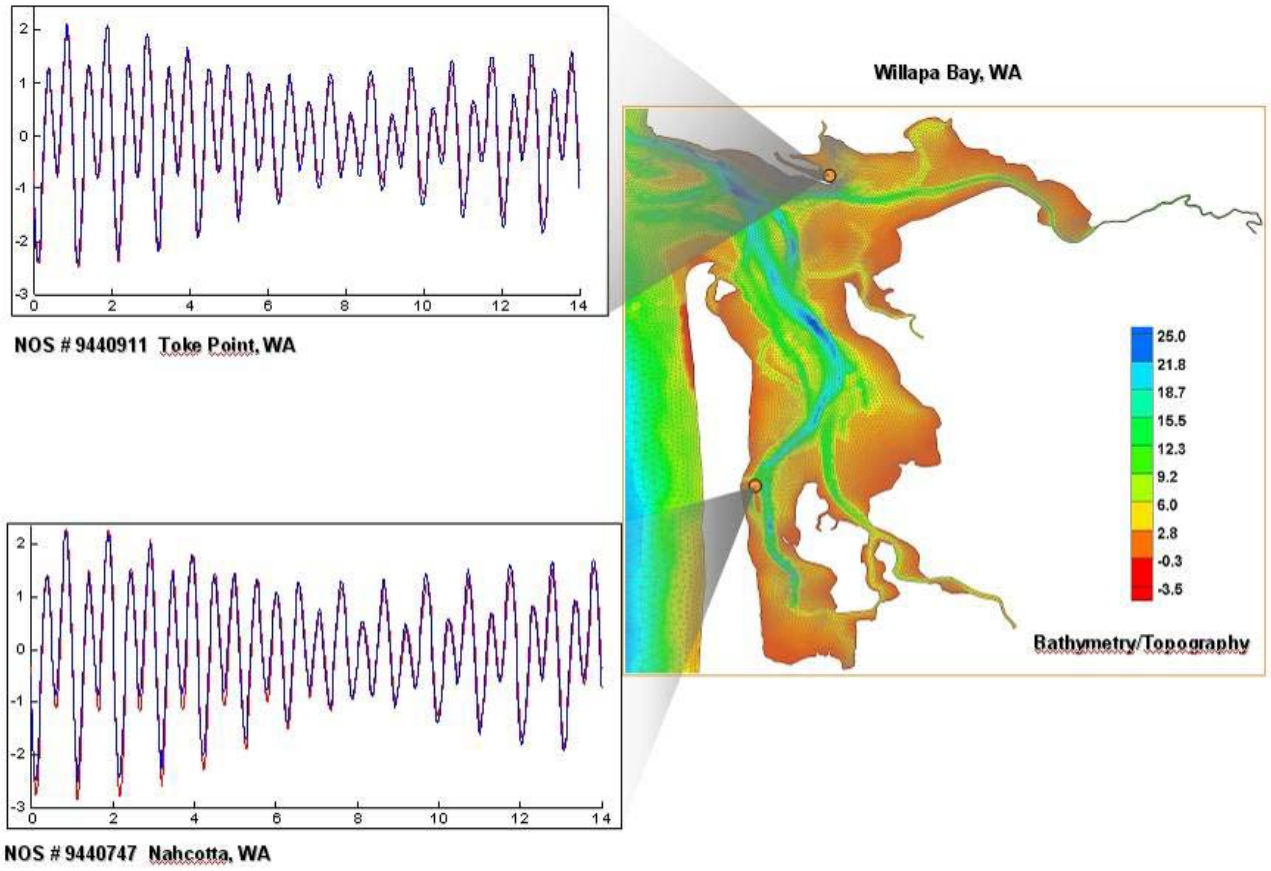

Figure 6: Willapa Bay tidal validation comparing model tides and Fourier re-synthesized measured tidal data.

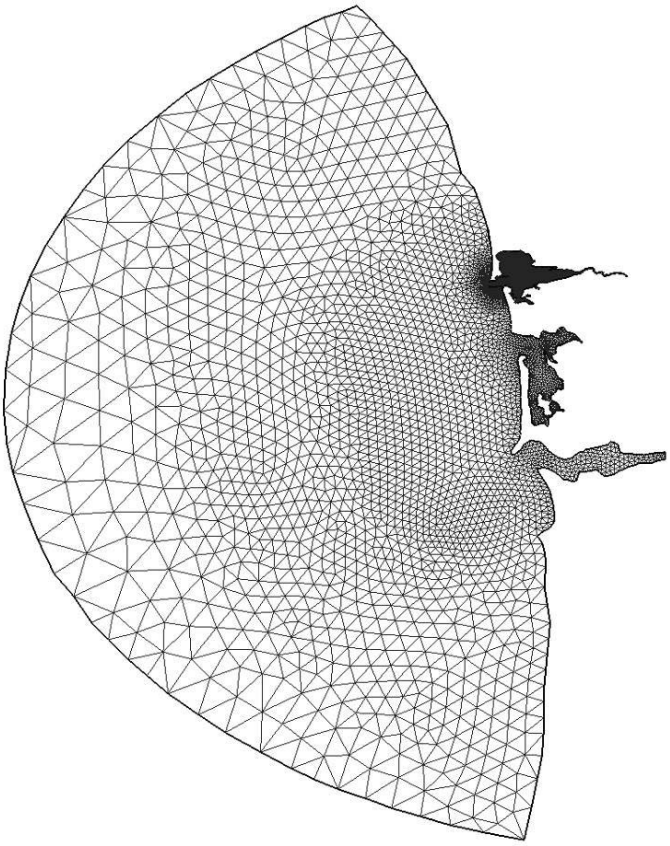

Figure 7: Grays Harbor p-adaptivity testing to resolve eddy features around jetties.

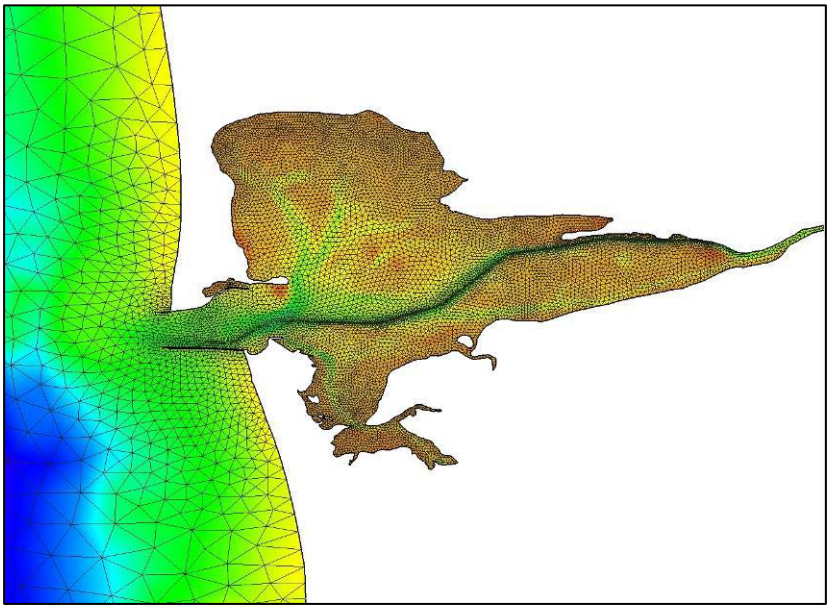

Figure 8: Grays Harbor grid and bathymetric detail.

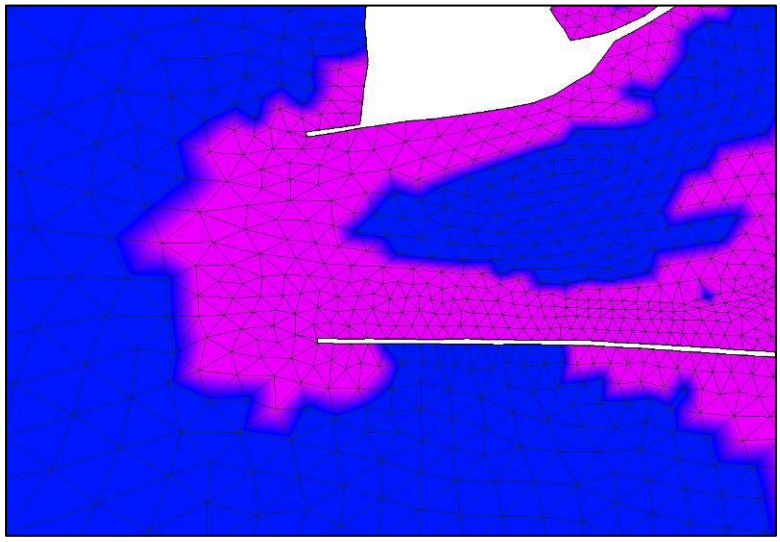

Figure 9: Grays Harbor p-adaptivity showing p=3 elements in purple and p=1 elements in blue on the flood tide.

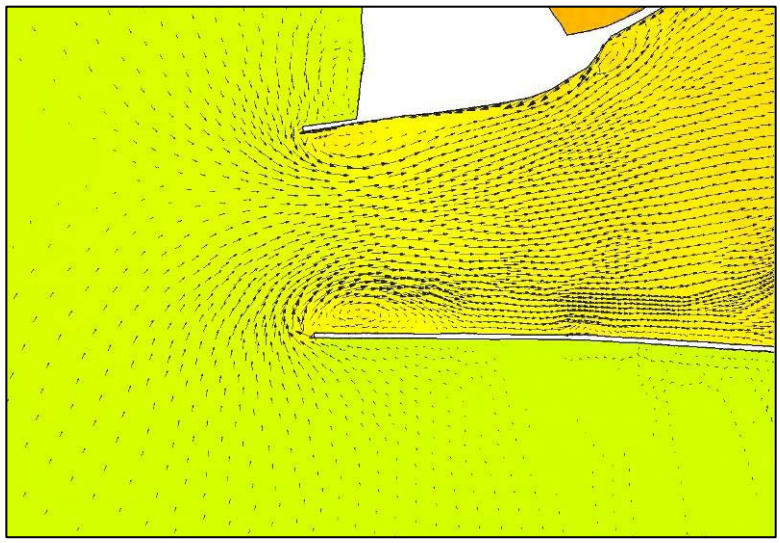

Figure 10: Grays Harbor p-adaptivity showing surface water elevations and current vectors on the flood tide.

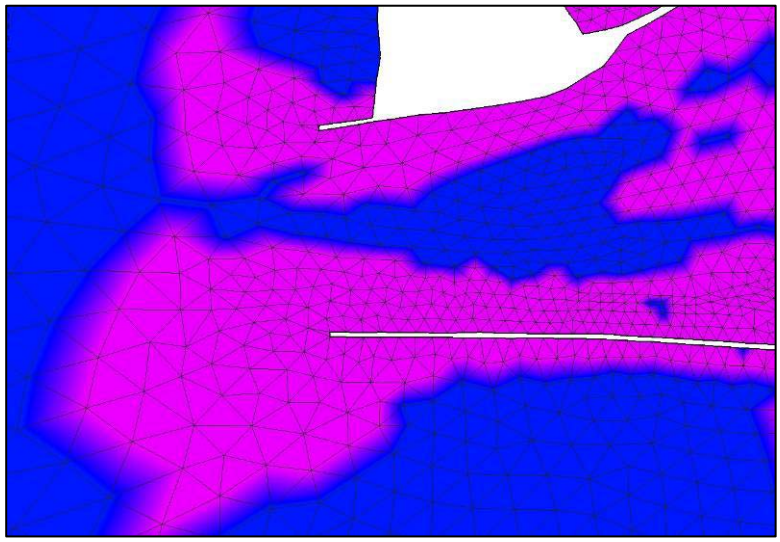

Figure 11: Grays Harbor p-adaptivity showing p=3 elements in purple and p=1 elements in blue on the ebb tide.

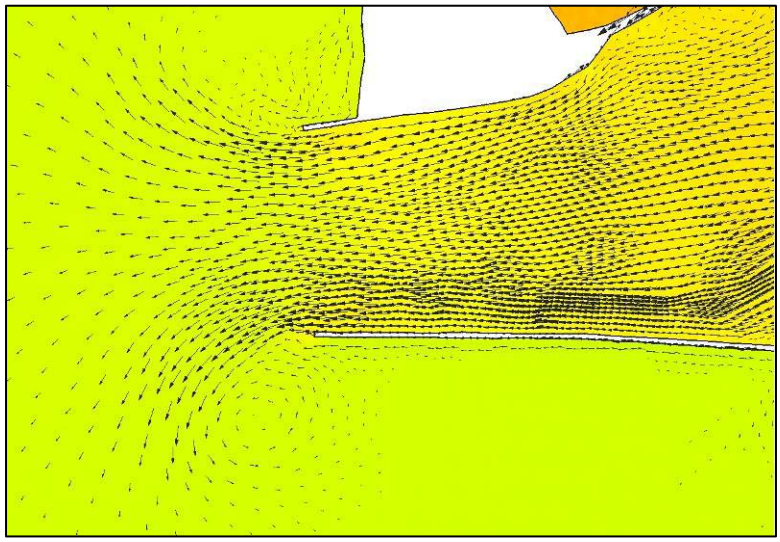

Figure 12: Grays Harbor p-adaptivity showing surface water elevations and current vectors on the ebb tide

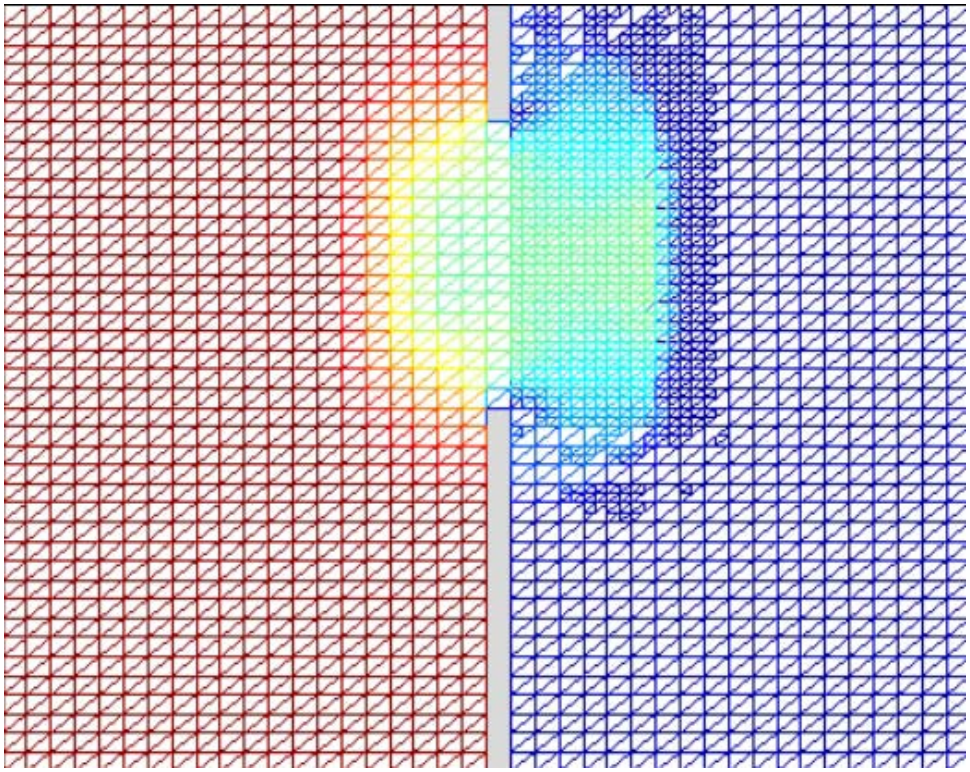

Figure 13: Idealized dam break problem with levels of h-adaptivity and colors indicating water level.

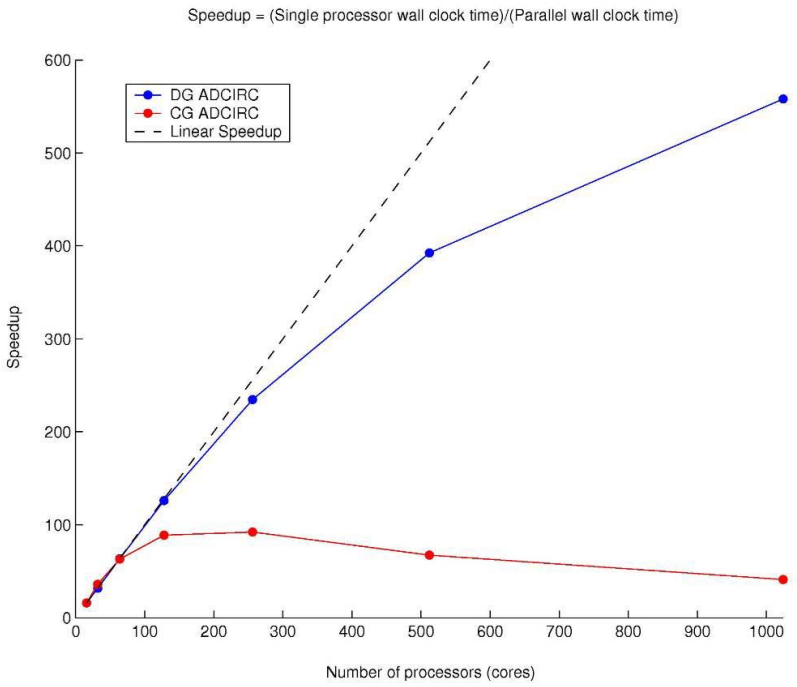

Figure 14: Idealized parallel speedup of the ADCIRC-CG and ADCIRC-DG codes up to 1024 cores for a 492,179 element model.

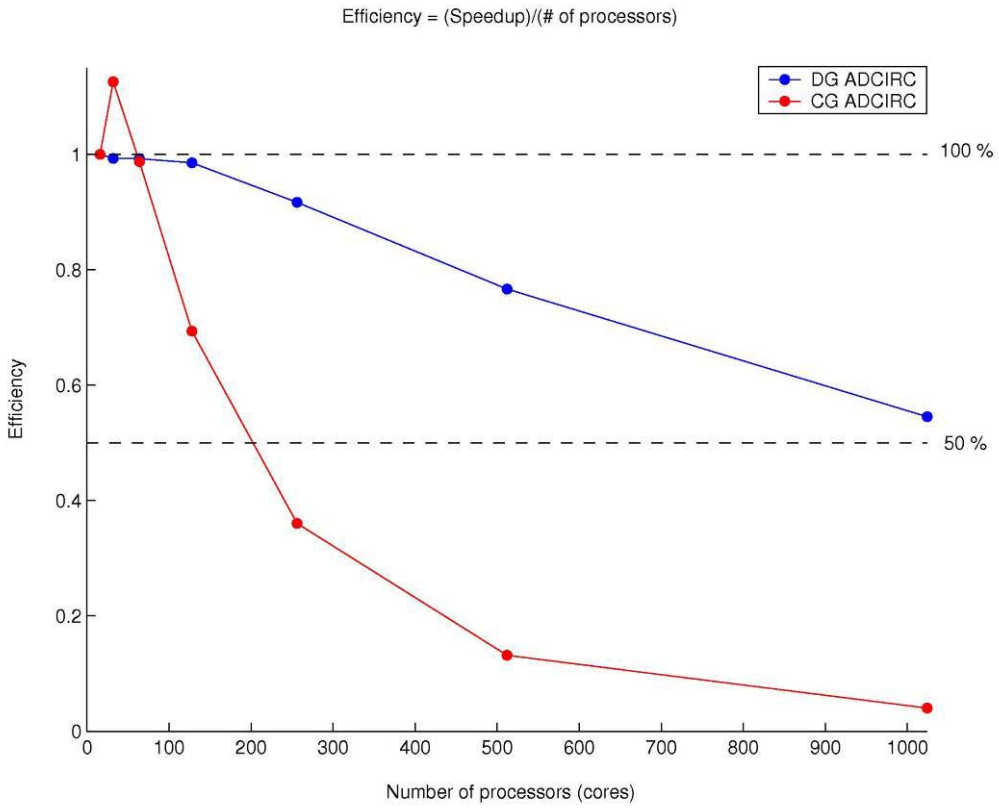

Figure 15: Parallel efficiency of the ADCIRC-CG and ADCIRC-DG codes up to 1024 cores for a 492,179 element model.

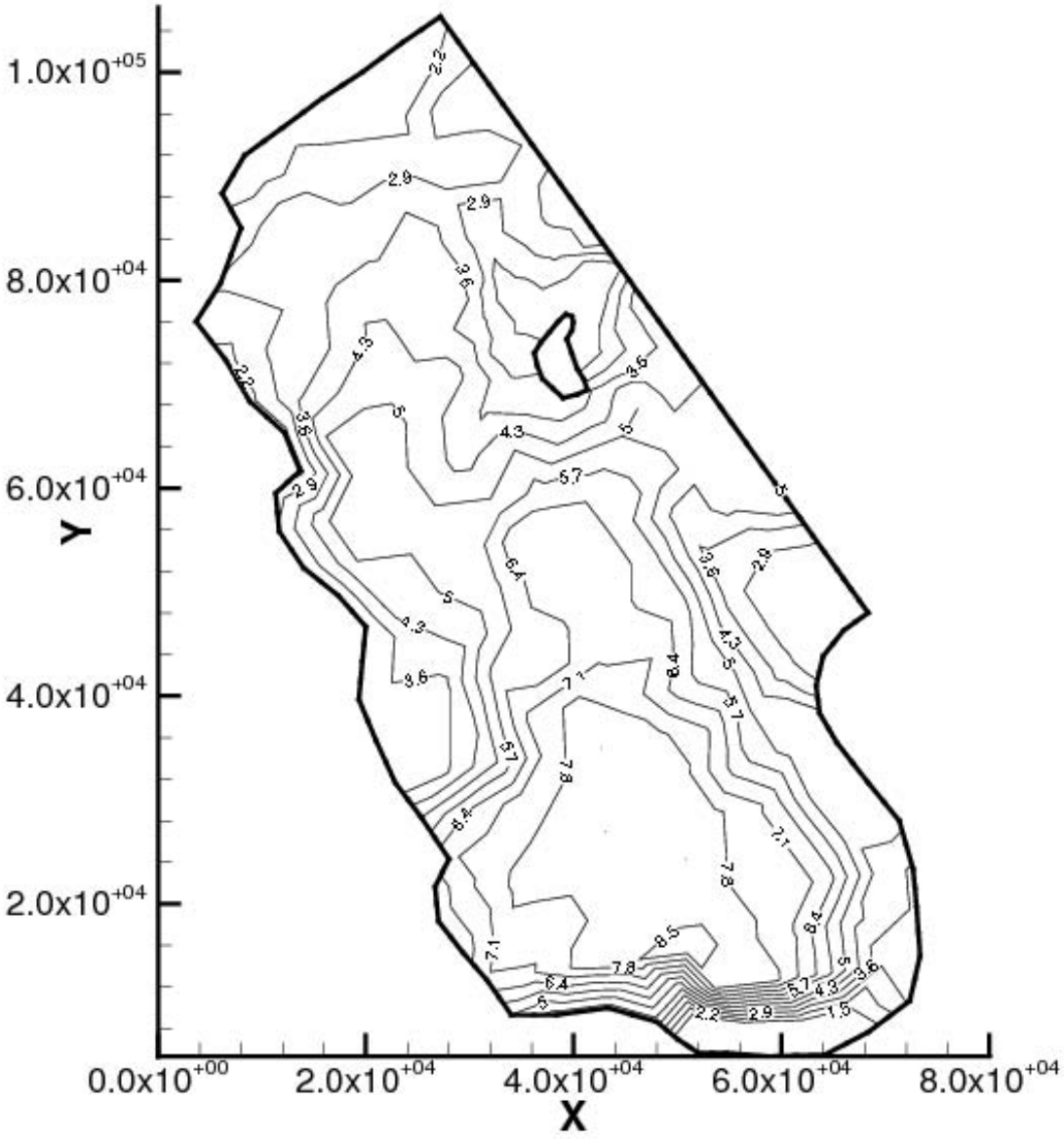

Figure 16: Bathymetry of the Bight of Abaco, Bahamas.

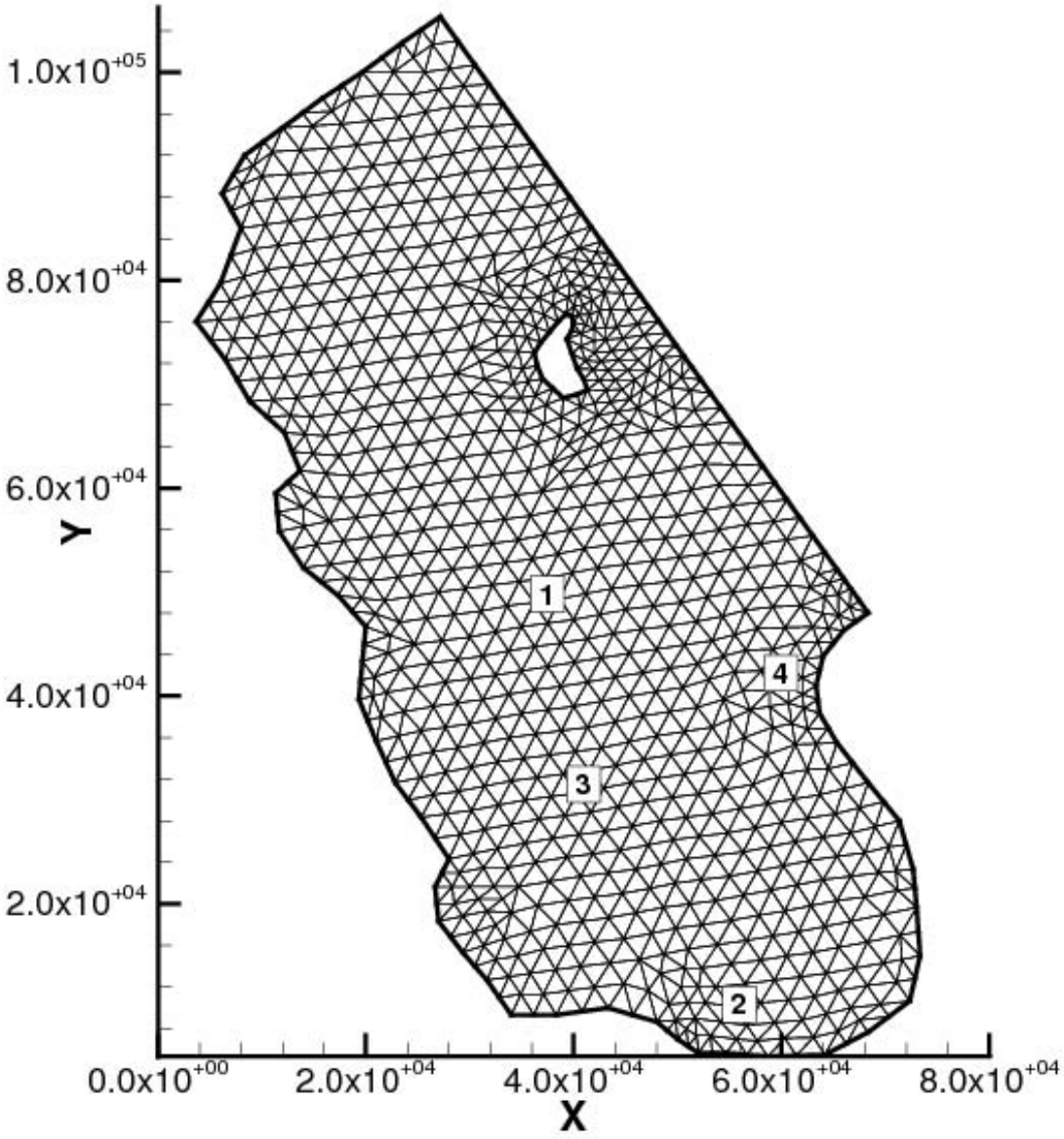

Figure 17: Finite Element grid of the Bight of Abaco, Bahamas.

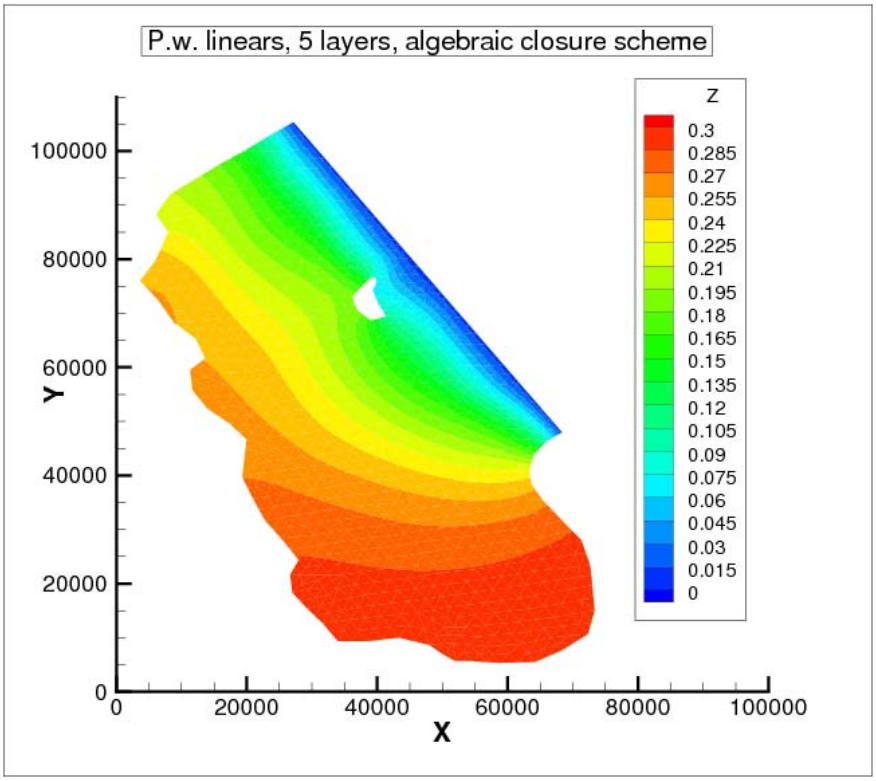

Figure 18: Free surface elevation at t=1,000,000 seconds in the Bight of Abaco using algebraic closure.

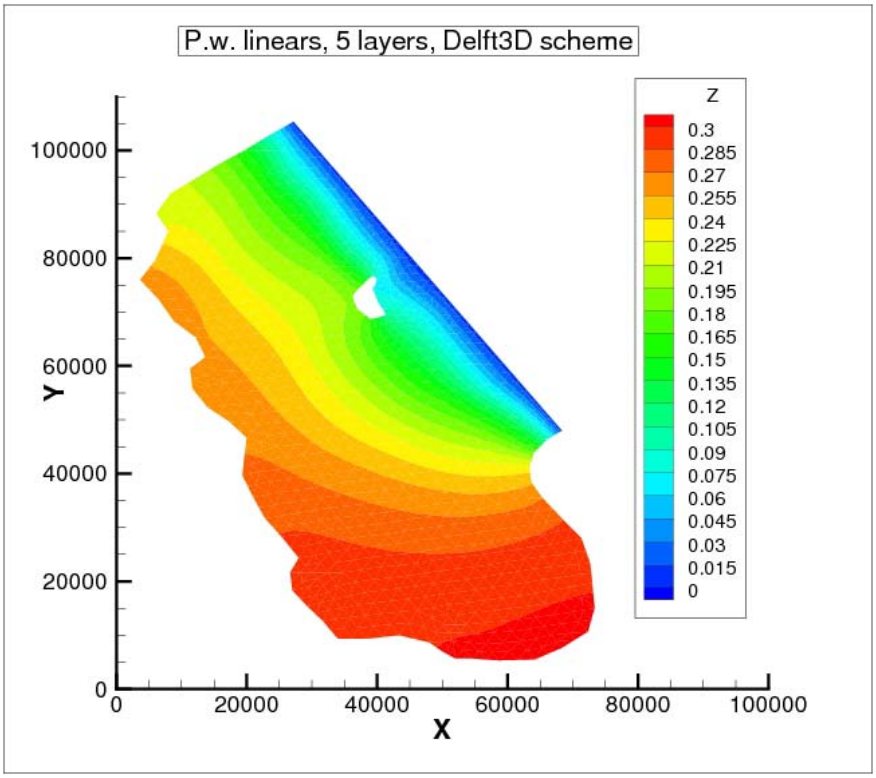

Figure 19: Free surface elevation at t=1,000,000 seconds in the Bight of Abaco using Delft 3D order 1 closure.

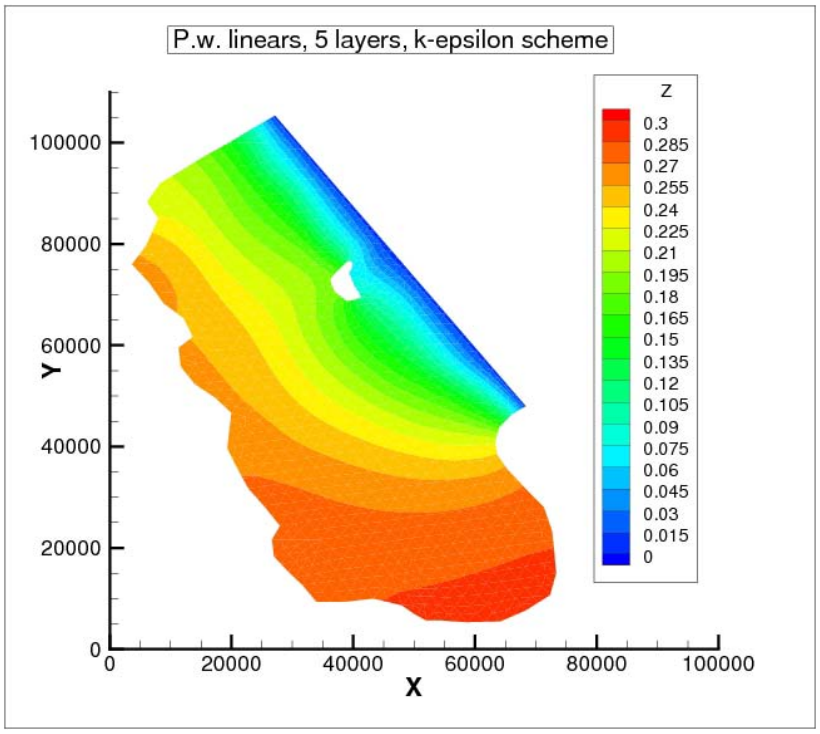

Figure 20: Free surface elevation at t=1,000,000 seconds in the Bight of Abaco using k-epsilon closure.

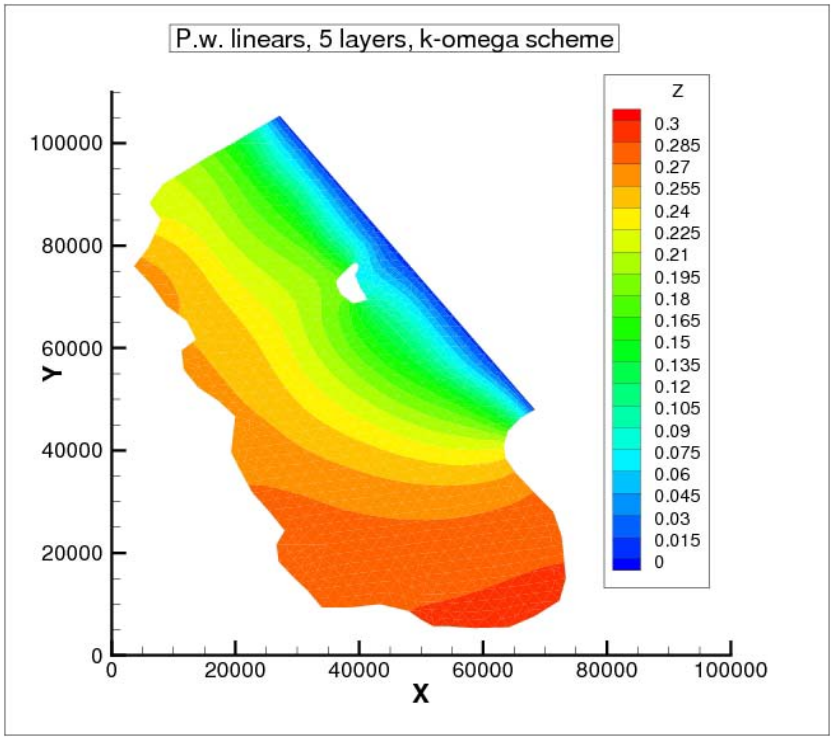

Figure 21: Free surface elevation at t=1,000,000 seconds in the Bight of Abaco using k-omega closure.

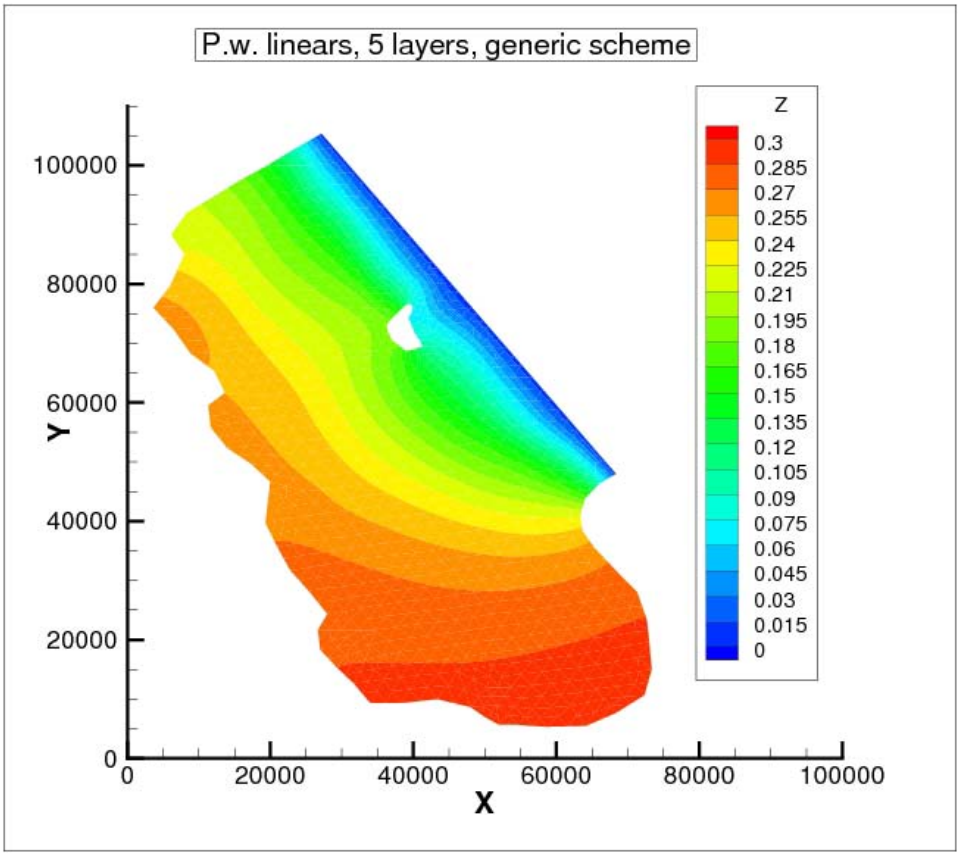

Figure 22: Free surface elevation at t=1,000,000 seconds in the Bight of Abaco using the generic order 2 closure.

.

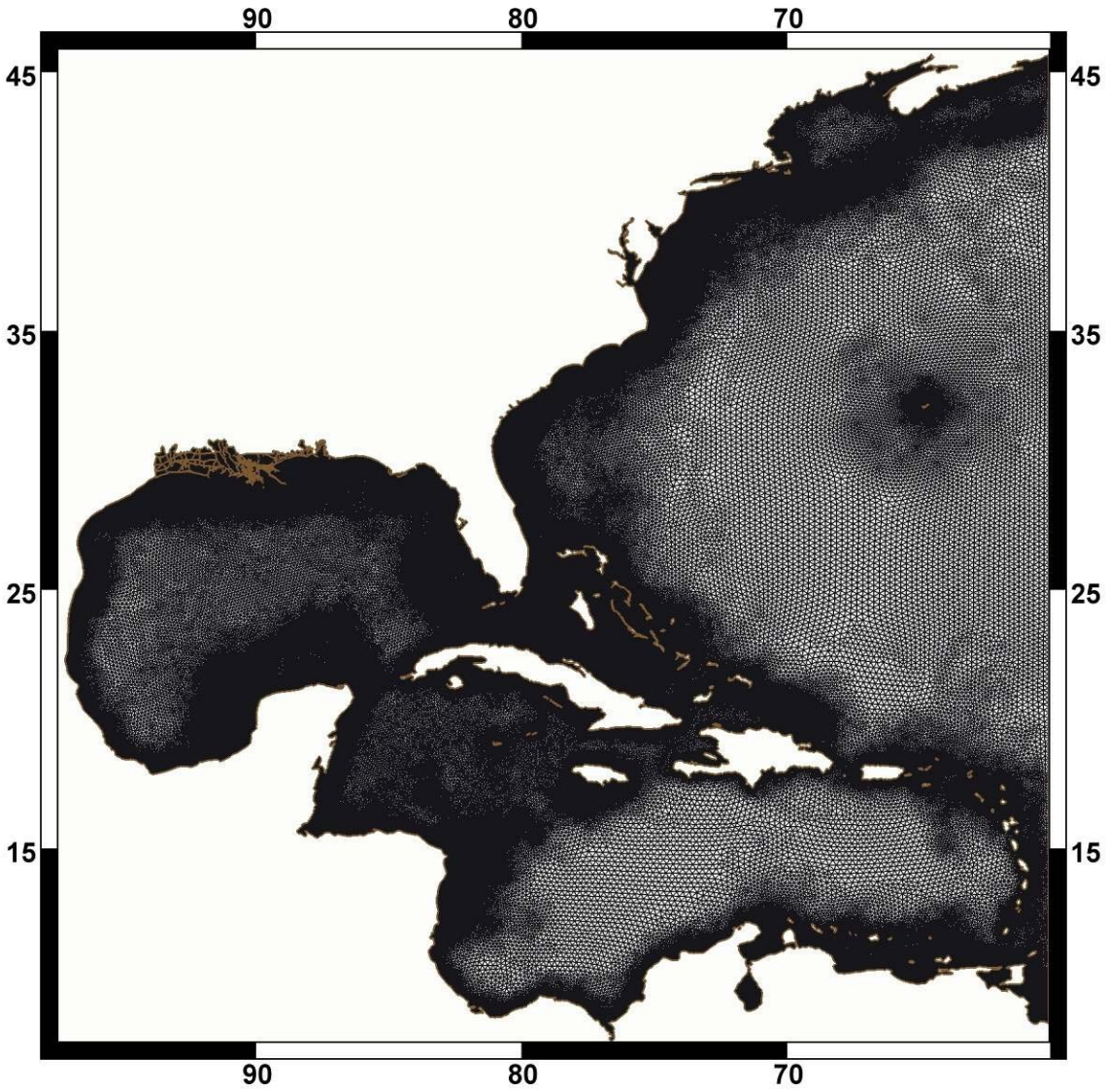

Figure 23: SL15 Computational domain and finite element grid for studying riverine, tidally, storm surge and wave radiation stress gradient induced flow in Louisiana and Mississippi.

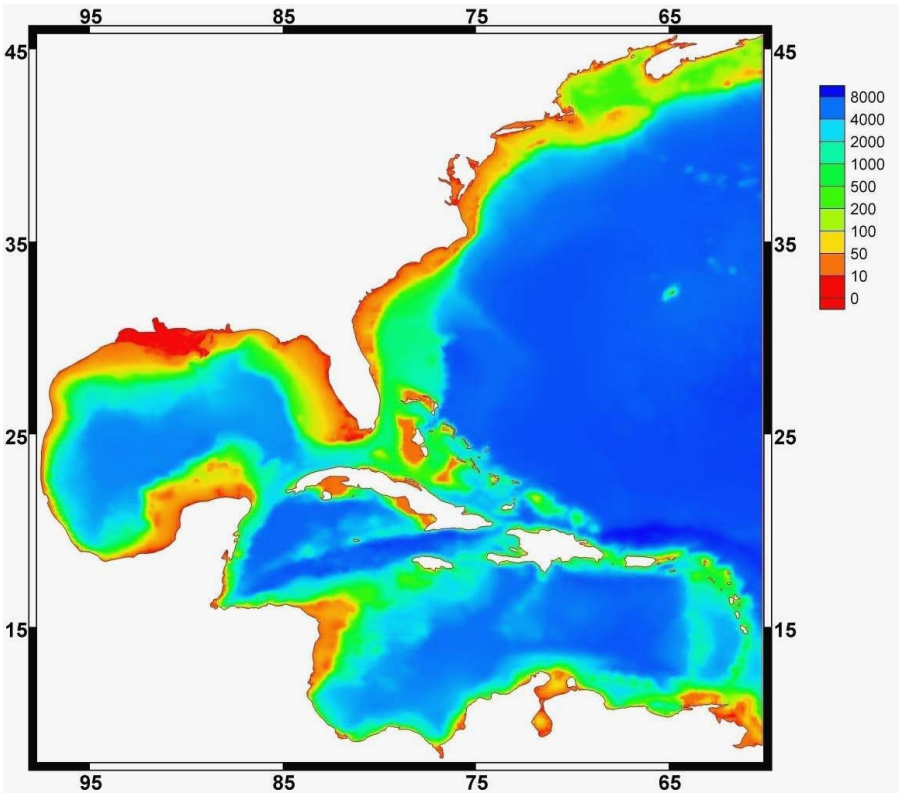

Figure 24: SL15 bathymetry for studying studying riverine, tidally, storm surge and wave radiation stress gradient induced flow in Louisiana and Mississippi.

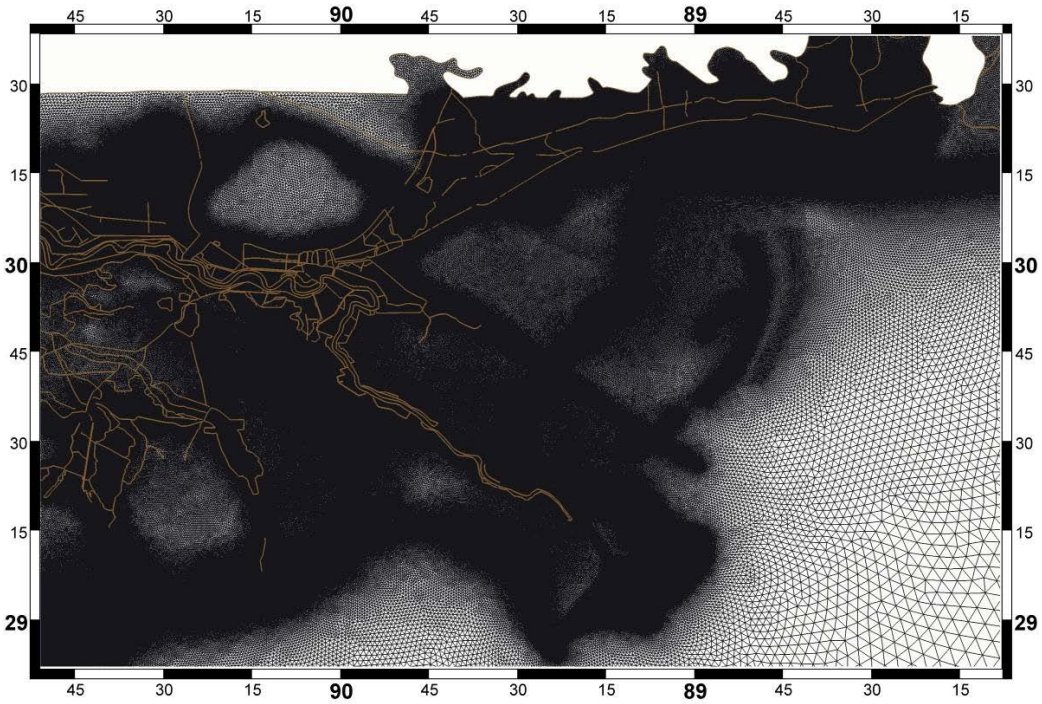

Figure 25: SL15 Computational grid detail for studying riverine, tidally, storm surge and wave radiation stress gradient induced flow in eastern Louisiana and western Mississippi.

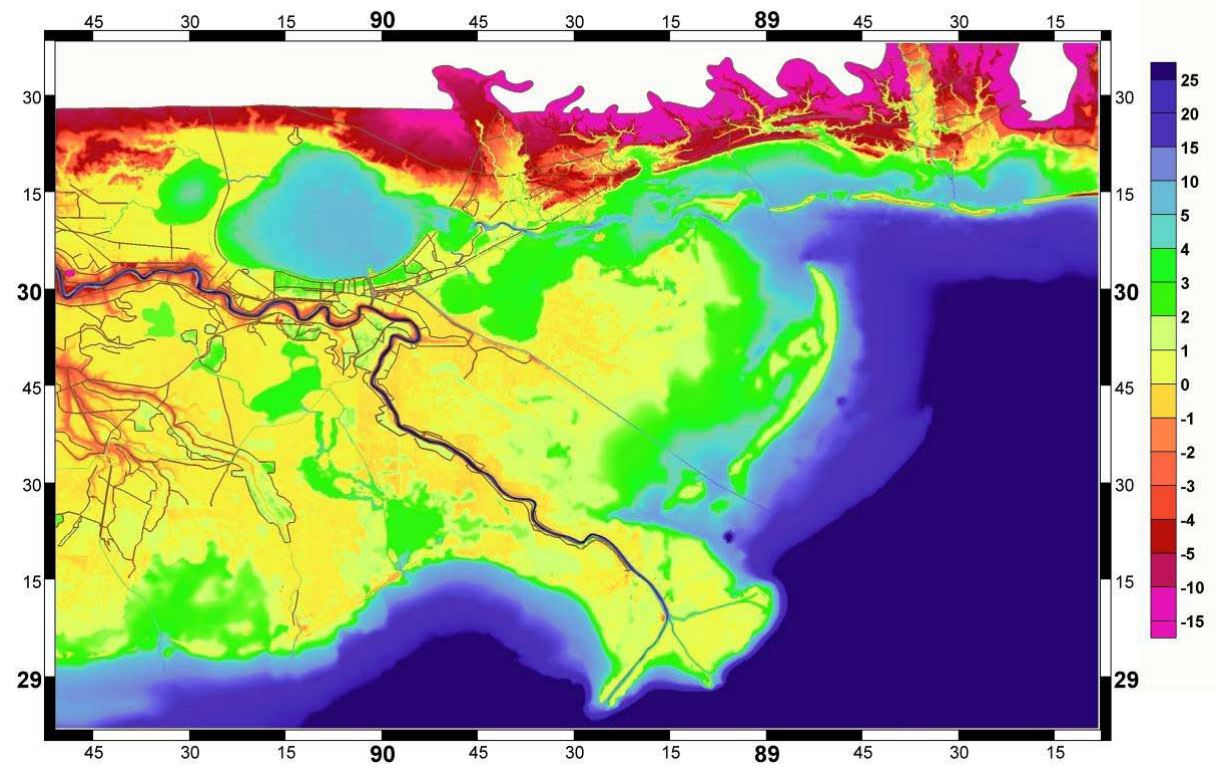

Figure 26: SL15 bathymetry and topography for studying riverine, tidally, storm surge and wave radiation stress gradient induced flow in eastern Louisiana and western Mississippi.

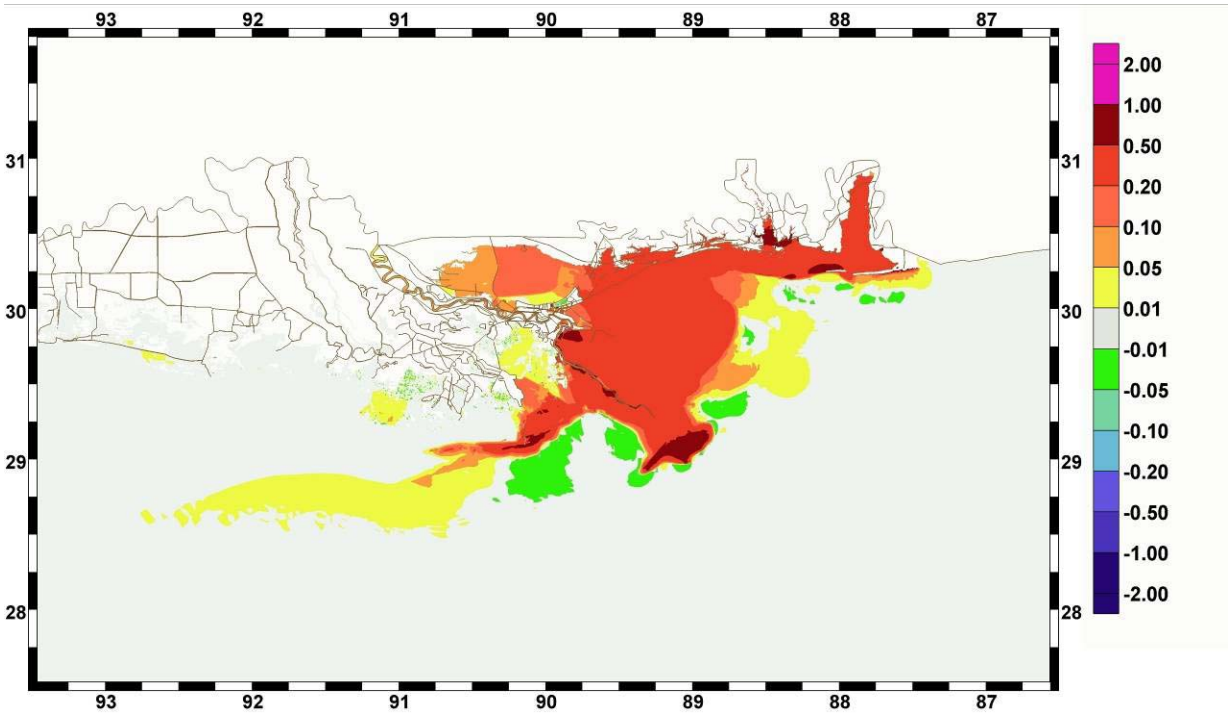

Figure 27: Computed wave radiation stress induced set up for eastern Louisiana and western Mississippi during Hurricane Katrina.

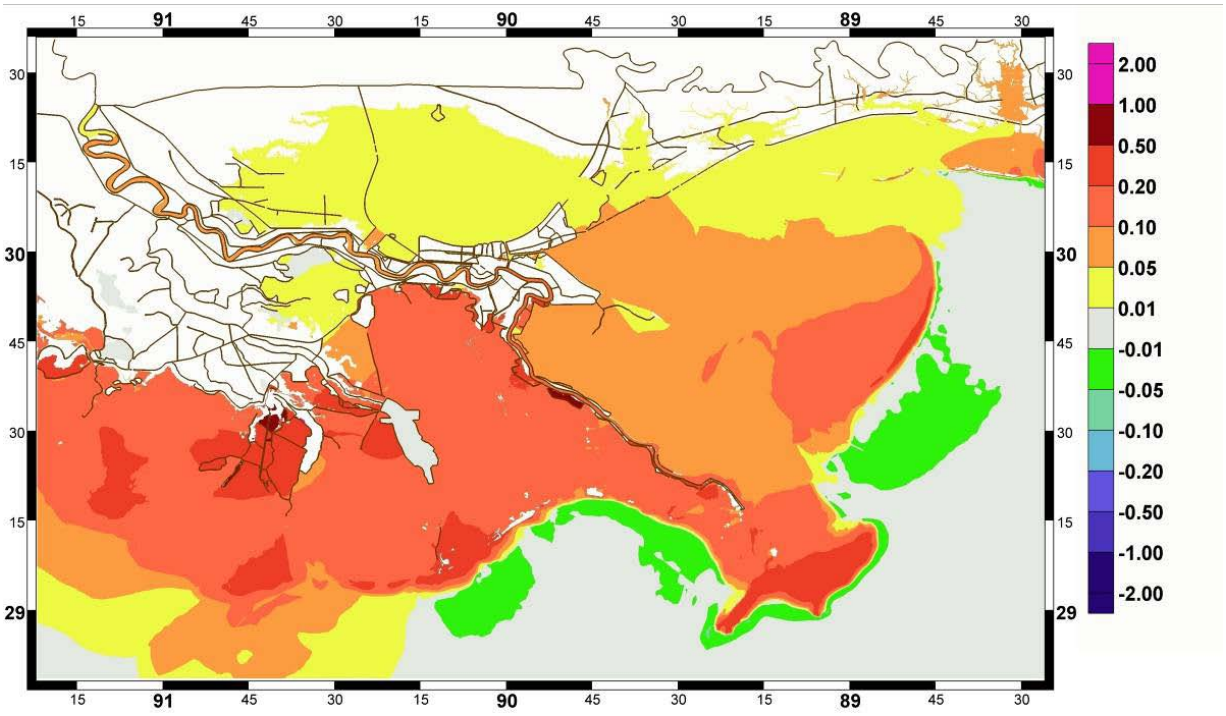

Figure 28: Computed wave radiation stress induced set up for eastern Louisiana and western Mississippi during Hurricane Rita.

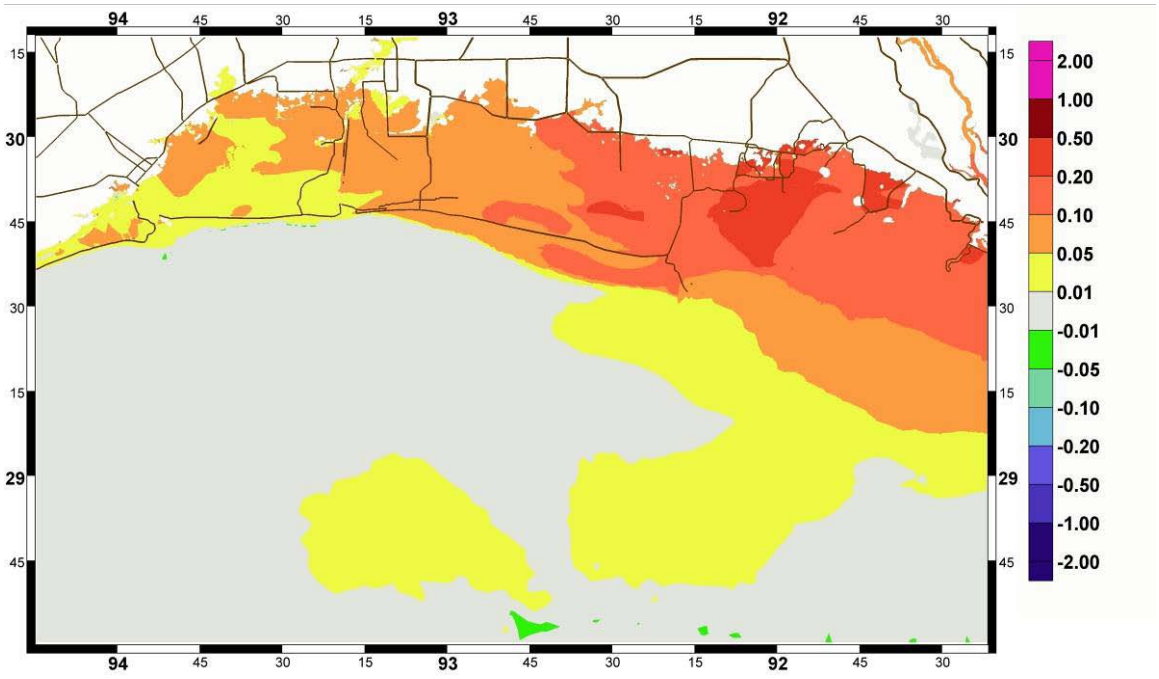

Figure 29: Computed wave radiation stress induced set up for western Louisiana during Hurricane Rita.